
Computations of premixed turbulent flames

M. Lecanu¹, K. Mehravaran¹, J. Fröhlich¹, H. Bockhorn¹, and D. Thévenin²

¹ Institute for Technical Chemistry and Polymer Chemistry, University of Karlsruhe, Germany, lecanu@ict.uni-karlsruhe.de

² Laboratory of Fluid Dynamics and Technical Flows, University of Magdeburg “Otto von Guericke”, Germany.

1 Motivation

Until now and at least for the next few decades, combustion is and will be the major source of mechanical and electrical energy. For economic and ecological reasons, it is of primordial interest to master phenomena involved in a very important number of processes using combustion. The SFB 606, a german research initiative on unsteady combustion, established at the University of Karlsruhe aims to improve the understanding and control of such processes. The research program is divided into several parts dedicated to the study of fundamental phenomena. One numerical part of SFB 606, Project B8 is devoted to the investigation of effects of differential diffusion on the propagation of flames in premixed gas. These are characterized by the Lewis number which is the ratio between diffusion of heat and mass, respectively. The goal of the present research is to understand these mechanisms by using Direct Numerical Simulations (DNS) in comparison with related experiments also realized in Karlsruhe within SFB 606. This will eventually allow comparison and close cross-validation. Such studies are the basis of modeling reactions in simulations of turbulent premixed flames and could be used in less costly numerical approaches such as statistical models or Large Eddy Simulation. In DNS, no model for turbulence is used and all the different length scales of the flow are computed, from the smallest in the flame front until the very large vortex structures. For these reasons the resolution demands are very high and hence the required CPU time. The present calculations in 2-D have been performed on the HP XC1 Cluster at the Karlsruhe Super Computing Center.

1.1 Relevance for premixed flames

In a wide range of the physical parameters, the effect of turbulence on a premixed flame is not limited to the wrinkling of the flame front. For example, when a flame front is submitted to sufficiently strong aerodynamic stretch,

quenching may appear locally and completely suppress the combustion process. Weaker turbulence, on the other hand, increases the propagation velocity of the flame front. From experimental data [1] or theoretical analysis, a first standard model of turbulent flame speed S_T is

$$\frac{S_T}{S_L} = 1 + \alpha \left(\frac{u'}{S_L} \right)^n \quad (1)$$

where S_L is the laminar flame speed, u' is the root-mean-square (rms) of the velocity fluctuations. α and n are model constants close to unity. This is a relatively simple model, though, which neglects all other effects. A more sophisticated model was proposed by Schmid [2] :

$$\frac{S_T}{S_L} = 1 + \frac{u'}{S_L} \left(\frac{Da_T^2}{1 + Da_T^2} \right)^{\frac{1}{4}}, \quad (2)$$

where Da_T is the turbulent Damköhler number.

Unfortunately, these models are limited and other factors, such as the flame front curvature become important when the Lewis number is different from unity. These Lewis number effects, also known as thermo-diffusive effects, will be studied in the present project. Special attention will also be paid to effects of flame curvature and stretch. Furthermore, the flame in turn affects the turbulence and a universal model should include this as well. To study the effects cited, it is mandatory to treat the full chemical system of reactions with all intermediate species, or at least a very good approximation of it, which then also involves many species. For each species a separate transport equation has to be solved and the chemical source terms have to be evaluated.

1.2 Experiments of Zarzalis in the framework of SFB 606

The experimental setup of Weiss and Zarzalis, investigated in Projekt A9 of SFB 606, is considered as a basis for the present simulations. These experiments investigate isochoric premixed spherical flames, evolving in a cubic box (Fig. 1). The burning velocity and the Markstein number are determined. The Markstein number Ma is a suitable parameter to quantify the influence of flame stretch and has to be included in the modeling of turbulent flame velocity [3, 4, 5].

1.3 Parameter range

The volume of the vessel used in the experiment is 2.3 l and the internal pressure can be raised up to 80 or 150 bar, depending on whether the optical access is used or not. So far, $H_2 - Air$ and $CH_4 - Air$ premixed laminar and turbulent flames with different initial compositions have been investigated

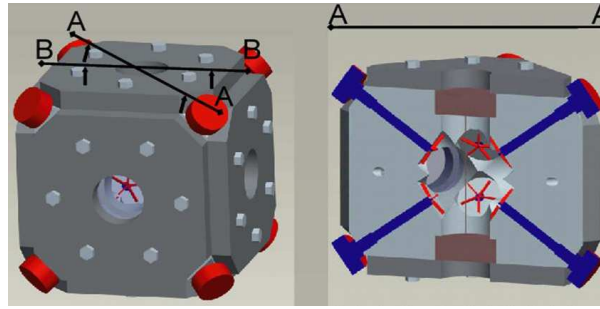


Fig. 1. Experimental setup of Weiss and Zarzalis - Project A9.

with this device. The gas mixture is ignited by a spark, located in the center of the box. Turbulence is generated and maintained with the use of eight fans located at the corners of the cubic box. The range of the turbulent fluctuations intensity is 0-4m/s. The Markstein number can be measured with a Schlieren method.

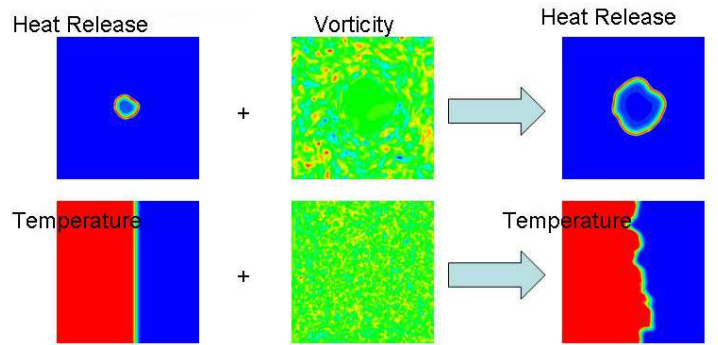


Fig. 2. Generation of initial conditions. Top row: ignition of a circular planar flame in a turbulent flow field. Bottom row: superposition of a turbulent flow field and of an initially plane flame front.

1.4 Flow configurations

The present work is concerned with 2-D configurations of premixed flames. The main parameters of the simulations are :

Thermochemistry :
 H_2 -Air mechanism, 9 species / 37 steps
 CH_4 -Air mechanism, 50 species / 300 steps

Initial conditions :

Two kinds of calculations with different initial conditions have been performed (Fig. 2). These are 2-D spherical flames and 2-D planar flames. Here, the second configuration is discussed. Its initial condition consists of a 1-D steady state solution obtained using the 1-D code *Premix* (employing the library Chemkin). This solution is extended to a 2-D laminar plane flame. The turbulent flow field is obtained from a 2-D turbulent kinetic energy spectrum. Velocity and concentration field are then superimposed.

Domain and grid :

We consider a square computational domain of $1\text{cm}\times 1\text{cm}$, discretized with an equispaced grid in both directions, typically of 501×501 points.

Boundary conditions :

Periodic boundary conditions are used along the planar flame, while non-reflecting boundary conditions are used in the direction normal to the flame on inflow and outflow boundaries. The calculations are initialized with reactants on one side of the computational domain and products on the other; they are separated by a laminar premixed flame.

CPU costs :

For a 2-D planar flame simulation consisting of 501×501 grid points with *H₂-Air* mechanism, the calculation of 1000 time steps typically takes 187 minutes for the serial computation, while an 8 processor run takes 30 minutes for the same number of iterations. The efficiency of the parallel simulations is discussed in the next part.

2 Numerical method

The direct numerical simulation approach consists of solving the Navier-Stokes equations in their complete form, without any averaging or filtering accounted for by a model. The code employed for this task is the code *Parcomb*, developed by Thévenin and co-workers [6].

Apart from the equations for continuity, momentum and energy, N_s equations are solved for the transport of chemical species, with $N_s = 9$ in the present cases. High-order discretization is used in order to reduce numerical dissipation. In space, this is a sixth order central finite-difference scheme along with a third order differencing at the boundaries. In time, a fourth-order Runge-Kutta scheme is employed. The Navier-Stokes characteristic boundary conditions [7, 8] are implemented taking into account detailed chemistry and thermodynamics.

Isotropic turbulence is generated in Fourier space with a von Kármán energy spectrum with Pao correction [9]. In Fourier space, the definition of the kinetic energy $E(k)$ is given by :

$$E(k) = A \frac{u'^5}{\varepsilon} \frac{\left(\frac{k}{k_e}\right)^4}{\left[1 + \left(\frac{k}{k_e}\right)^2\right]^{\frac{17}{6}}} \exp\left[-\frac{3}{2} \alpha \left(\frac{k}{k_d}\right)^{\frac{4}{3}}\right] \quad (3)$$

where k is the wave number, u' the rms value of velocity fluctuations, ε is the dissipation, while A and α are constants of the model ($A = 1.5$ and $\alpha = 1.5$). Furthermore,

$$k_e = 1/L_e, \quad (4)$$

where L_e is the peak energy wavelength, and

$$k_d = 1/L_d, \quad (5)$$

where L_d is the Kolmogorov wavelength. After the initialization, no forcing of the turbulent flow field is applied and the fluctuations are allowed to decay. The propagation of the flame is relatively fast, however, so that this decay is not too strong. Examples of calculations with *Parcomb* and postprocessing intended towards turbulent combustion modeling are available in [10, 11, 12].

3 Issues of HPC

3.1 Parallelization : PVM versus MPI

Parcomb is a fully parallel program with dynamic load balancing capabilities. The message passing library originally used in *Parcomb* is PVM. All the validations performed by the authors was also using PVM. Thus, it was natural to continue using the program with PVM. PVM, however, is now superseded by MPI and no more maintained on current installations. Hence, in a first phase of the project it was converted to MPI and fully tested and validated on the XC using HP-MPI.

An attempt to use MPI instead of PVM in *Parcomb* had been made previously during the development, using wrappers around the PVM calls. However, this revision was not validated and could not be compiled with the present installation. Most of the parallelization calls were therefore rewritten. Tests with MPICH and HP-MPI served to avoid lacks of portability. The communication of the number of processors in each direction to all processes may serve as an example. The sets of original calls

```
PVMFINITSEND
PVMFPACK
PVMFMCAST
```

coupled with the receiving instructions:

PVMFREC
PVMFUNPACK

were replaced by a single

MPI_BCAST

instruction. Since these blocking instructions are in the initialization part, they do not reduce the overall performance of the code. The code was then thoroughly tested against the serial version, both in 1-D and 2-D configurations and using different numbers of processors.

3.2 Efficiency of runs

Benchmarking of the code was performed with a 2-D reacting configuration. The test case used corresponds to the 2-D ignition of a turbulent premixed hydrogen-air flame. Timings are presented for a scaled problem, which means that all nodes possess the same number of grid points (201×201 points and a $7\text{mm} \times 7\text{mm}$ domain). When increasing the number of processors, the size of the domain and the total number of grid points are increased proportionally. The simplest definition of the parallel efficiency is used here, i.e. $E(N) = t_{CPU}(1)/t_{CPU}(N)$, where N is the number of processors. Since dual nodes were employed only even numbers were chosen.

Efficiency results are given in Figure 3(a) and corresponding CPU times are shown in Figure 3(b). These data show that the parallelization performs very well, with generally no decrease in the performance when using more processors. Of course, these results should not be used as a direct measurement of the performance of the machine, but they can give some insights about the practical achievement of *Parcomb* on the XC.

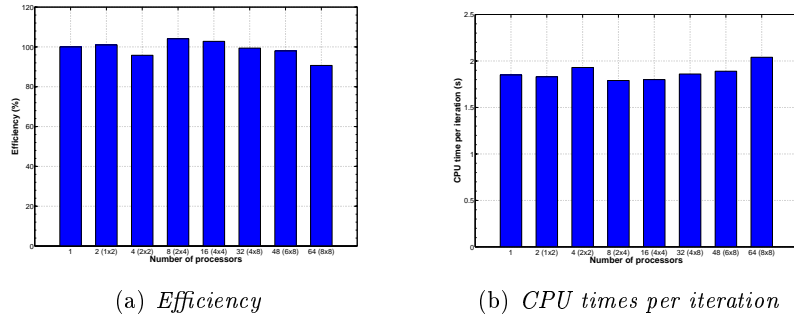


Fig. 3. Dependence of efficiency (left) and CPU time per time step (right) on the number of processors.

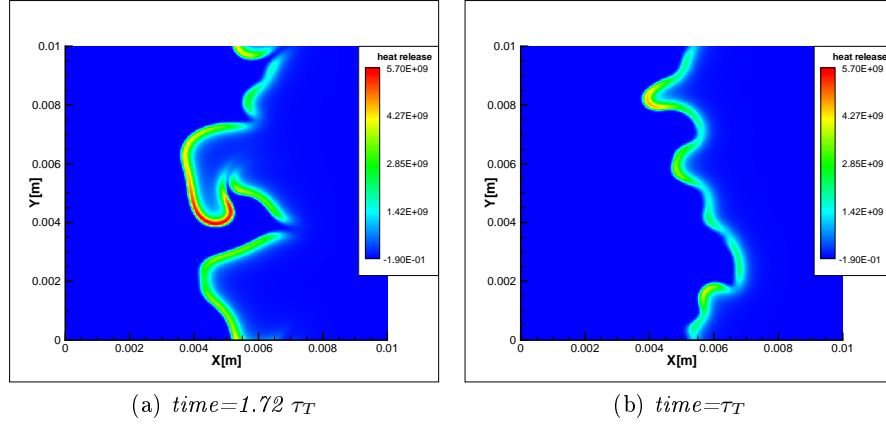


Fig. 4. Heat release contours. Case 1 on the left : $u'/S_L = 7.4$, $\Lambda/\delta_l = 15.4$ - Case 2 on the right : $u'/S_L = 2.5$, $\Lambda/\delta_l = 2.5$.

4 Sample results

Results of two calculations are presented in this section. We considered a lean premixed H_2 -*Air* 2-D turbulent flame ($\lambda = 2$). The grid has 500×500 points. Two different initial flow fields have been used :

Case 1 :

rms-value of velocity fluctuations $u' = 4.95 \text{ m/s}$, turbulent integral length scale $\Lambda = 6 \cdot 10^{-3} \text{ m}$, turbulent Reynolds number $Re = 1853$, eddy turnover time $\tau_t = \Lambda/u' = 1.22 \cdot 10^{-3} \text{ s}$, laminar flame thickness $\delta_L = 3.9 \cdot 10^{-4} \text{ m}$, laminar flame speed $S_L = 0.67 \text{ m/s}$, $\tau_c = \delta_L/S_L = 5.82 \cdot 10^{-2} \text{ s}$.

Case 2 :

rms-value of velocity fluctuations $u' = 1.68 \text{ m/s}$, turbulent integral length scale $\Lambda = 9.7 \cdot 10^{-4} \text{ m}$, turbulent Reynolds number $Re = 101$, eddy turnover time $\tau_t = \Lambda/u' = 0.98 \cdot 10^{-3} \text{ s}$, laminar flame thickness $\delta_L = 3.9 \cdot 10^{-4} \text{ m}$, laminar flame speed $S_L = 0.67 \text{ m/s}$, $\tau_c = \delta_L/S_L = 5.82 \cdot 10^{-2} \text{ s}$.

Figure 4 illustrates the interaction between the flame front and two different turbulence fields. The higher turbulence level in Case 1 produces curvature, strain, stretch and even quenching on the flame front, which can be observed in figure 4(a). In contrast, the turbulence in Case 2 is weaker and solely wrinkling can be observed in the figure 4(b).

Theoretical studies suggest a linear relation between the displacement flame speed S_d and stretch for small amounts of stretch, i.e.

$$\frac{S_d}{S_L} = 1 - Ma Ka, \quad (6)$$

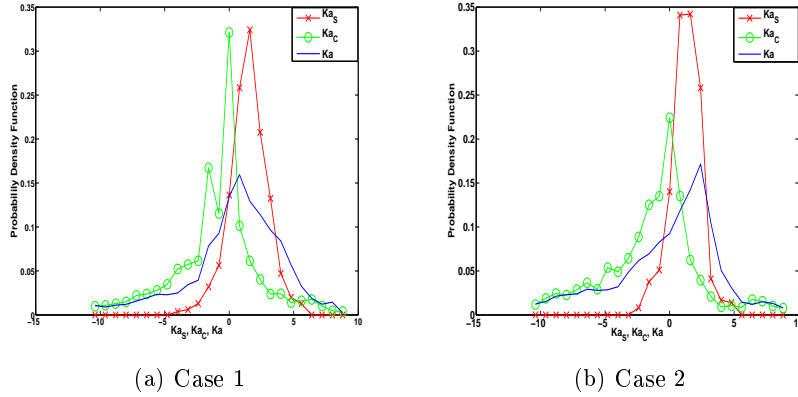


Fig. 5. Probability density functions of normalized stretch rate Ka (solid line), tangential strain rate Ka_S (circles) and curvature term of stretch Ka_C (crosses).

where S_L is the laminar flame speed and $Ka = \kappa\delta_F/S_L$ is the Karlovitz number or non-dimensional flame stretch by turbulence, while Ma is the Markstein number and δ_F is the nominal flame thickness. Flame stretch κ is defined as the sum of the tangential strain rate a_T and the curvature term.

$$\kappa = a_T + S_d\nabla \cdot n \quad (7)$$

where $\nabla \cdot n$ is the flame curvature and n is the flame normal vector. The Karlovitz number Ka can be written as the sum of the strain component and the curvature component :

$$Ka = \frac{\delta_F}{S_L}(a_T + S_d\nabla \cdot n) = Ka_S + Ka_C. \quad (8)$$

The following DNS results in Fig.5 and Fig.6 are used to evaluate the flame speed in terms of the displacement speed of the flame front. The isocontour $Y_{H_2} = 0.175$ has been used to represent the flame front as it corresponds to the maximum heat release contour. Statistics were then accumulated along this contour line. The shape of the total stretch rate Ka changes shape substantially with Reynolds number. For low Reynolds number (Case 2) its shape is inclined towards positive values, while for higher Reynolds number (Case 1) more negative values of Ka occur. The reason is provided by the decomposition: For low Re , the PDF of the curvature term is narrow and centered around a positive value. For higher Re it broadens without substantial shift of mean. The strain-rate contribution on the other hand narrows from low to higher Re .

Figure 6 displays cross-correlations along the flame front (again identified by the $Y_{H_2} = 0.175$ level line). Further simulations with different realizations

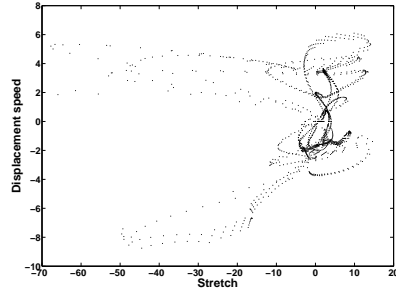
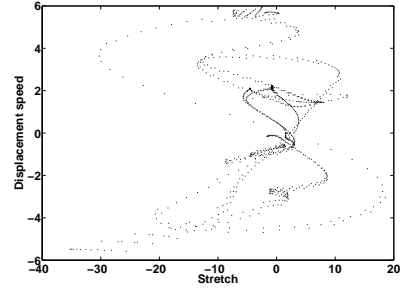
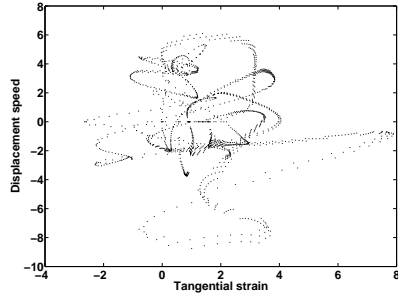
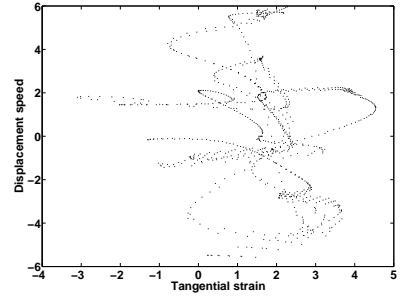
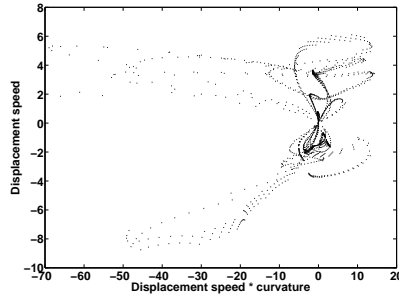
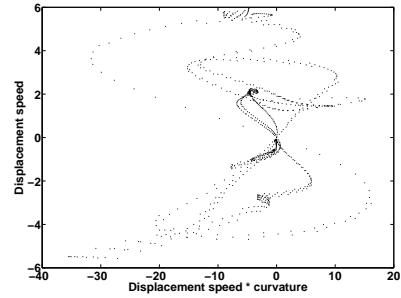

 (a) *Speed versus stretch.*

 (b) *Speed versus stretch.*

 (c) *Speed versus tangential strain.*

 (d) *Speed versus tangential strain.*

 (e) *Speed versus curvature term.*

 (f) *Speed versus curvature term.*

Fig. 6. Correlations of normalized displacement flame speed versus stretch rate, tangential strain rate and curvature term of stretch. Results are for Case 1 on the left, $u'/S_L = 7.4$ and for Case 2 on the right, $u'/S_L = 2.5$. Note the different scaling of the x -axis in Fig. 6(c) and 6(d).

of the same physical setup need to be performed in order to perform statistical averaging, but the graphs reported here allow already a first interpretation. Figures 6(a) and 6(b) show two distinct stable branches depending on the sign

of the displacement speed. This is in agreement with the observations of Chen and Im [13]. By comparing correlations of displacement flame speed versus tangential strain rate (Figs. 6(c) and 6(d)) and curvature term of stretch (Figs. 6(e) and 6(f)), it can be observed that the large negative values of stretch solely result from the curvature term Ka_C and not from Ka_S . This is in line with the discussion of Figure 5.

5 Conclusions

Within SFB 606, DNS calculations for turbulent flames in premixed gas have been performed with the parallel fortran code *Parcomb*. The present calculations allow a better understanding of phenomena involved in turbulent premixed combustion, such as differential diffusion, and will be used to evaluate the turbulent flame speed taking account stretching, wrinkling and quenching of the flame front.

In a first phase of the project, *Parcomb* has been converted to MPI. It also has been validated and tested using up to 64 processors showing very good parallel efficiency. Further 2-D simulations are under way to accumulate statistics and to elucidate Lewis effects in turbulent premixed flames. Several 3-D configurations will be studied afterwards.

Acknowledgements: Funding of the present research by the German Research Foundation (DFG) through SFB 606 is gratefully acknowledged. The required CPU time was kindly provided by the SCK Karlsruhe.

References

- [1] R.G. Abdel-Gayed and D. Bradley. Lewis number effects on turbulent burning velocity. *Proceedings of the Combustion Institute*, 20:505–512, 1984.
- [2] H.-P. Schmid, P. Habisreuther, and W. Leuckel. A model fo calculating heat release in premixed turbulent flames. *Combustion and Flame*, 113:79–91, 1998.
- [3] D. Bradley, P.-H. Gaskell, and X.-J. Gu. Burning velocities, Markstein lengths and flame quenching for spherical methane-air flames : a computational study. *Combustion and Flame*, 104:176–198, 1996.
- [4] T. Brutscher, N. Zarzalis, and H. Bockhorn. An experimentally based approach for the space-averaged burning velocity used for modeling premixed turbulent combustion. *Proceedings of the Combustion Institute*, 29:1825–1832, 2002.
- [5] D. Bradley, P.-H. Gaskell, X.-J. Gu, and A. Sedaghat. Premixed flamelet modelling : factors influencing the turbulent heat release rate source and the turbulent burning velocity. *Combustion and Flame*, 143:227–245, 2005.
- [6] D. Thévenin, F. Behrendt, U. Maas, B. Przywara, and J. Warnatz. Development of a parallel direct simulation code to investigate reactive flows. *Computers and Fluids*, 25:485–496, 1996.
- [7] T. Poinso and S. Lele. Boundary conditions for direct simulations of compressible viscous flows. *Journal of Computational Physics*, 101:104–129, 1992.
- [8] M. Baum, T. Poinso, and D. Thévenin. Accurate boundary conditions for multicomponent reactive flows. *Journal of Computational Physics*, 116:247–261, 1994.
- [9] J. O. Hinze. *Turbulence*. McGraw-Hill, 2nd edition, 1975.
- [10] J. De Charantenay, D. Thévenin, and B. Zamuner. Comparison of direct numerical simulations of turbulent flames using compressible or low-Mach number formulations. *International Journal For Numerical Methods In Fluids*, 39:497–515, 2002.

- [11] R. Hilbert and D. Thévenin. Influence of differential diffusion on maximum flame temperature in turbulent nonpremixed hydrogen/air flames. *Combustion and Flame*, 138:175–187, 2004.
- [12] D. Thévenin, P.-H. Renard, J. C. Rolon, and S. Candel. Extinction processes during a non-premixed flame/vortex interaction. *Proceedings of the Combustion Institute*, 27:719–726, 1998.
- [13] J.H. Chen and H.G. Im. Correlation of flame speed with stretch in turbulent premixed methane/air flames. *Proceedings of the Combustion Institute*, 27:819–826, 1998.